PCCP

Accepted Manuscript

ROYAL SOCIETY OF CHEMISTRY

www.rsc.org/pccp

Two-atom-thick semiconducting carbon sheet

Meng Hu, Yu Shu, Lin Cui, Bo Xu, Dongli Yu, Julong He*

State Key Laboratory of Metastable Materials Science and Technology, Yanshan University, Qinhuangdao 066004, China

* E-mail: hjl@ysu.edu.cn

Abstract

H-net, a two-dimensional (2D) carbon allotrope incorporating distorted squares C_4, hexagons C_6, and octagons C_8, is proposed using first principle calculations. Different from the previous planar graphene and other theoretical carbon sheets, H-net is a two-atom-thick polymorph with identical C_6+C_4+C_6 components cross facing and covalently buckled to feature a handshake-like model. The feasible existence of H-net is evident from its dynamic stability as confirmed by phonon-mode analysis and lower total energy. H-net is energetically more favorable than synthesized graphdiyne and theoretical graphyne, BPC, S-graphene, polycyclic net, α-squarographite, and lithographite. Therefore, we address a possible synthetic route from graphene nanoribbon. Electronic band structure calculations indicate that H-net is a semiconductor with an indirect band gap of 0.88 eV, whereas graphene and many 2D carbon sheets are metallic. We also explore the electronic structure properties of the one-dimensional derivative nanoribbons of H-net. The narrowest H-net nanoribbon exhibits metallic behavior, and the others are semiconducting with growing band gaps as nanoribbon widths. H-net and its tailored nanoribbons are expected to possess more properties than graphene because of their exceptional crystal structure and different energy band.

Keywords: two-dimensional carbon allotrope; two-atom thick; semiconducting

1 Introduction

Graphene is considered a promising materials due to its unique combination of exceptionally high electronic and thermal conductivities, extreme mechanical stiffness, strength and elasticity, and outstanding chemical durability.[1, 2] Consequently, graphene stimulates extensive investigations on the structural stabilities and electronic characteristics of new two-dimensional (2D) carbon sheets.[3-5] The identification of their intriguing properties is emergent for future generation nanoelectronics and photonics. Research on 2D graphyne and graphdiyne indicates that their electronic properties are even more remarkable and versatile than those of graphene because of their directional anisotropy and nonequivalent Dirac points.[6-9] Recently, large graphdiyne films have been realized through a cross-coupling reaction,[10] and this breakthrough further triggers burgeoning research interests on novel 2D carbon polymorphs.

To manipulate the atomic and electronic properties of graphene for broader applications, such as future post-silicon nanoelectronic devices, much attention has been paid on the exploration of introducing atomic-scale defects, such as various topological defects, atomic vacancies, or dislocations into integral graphene. Accordingly, novel non-hexagon polygon-constructed 2D planar carbon sheets are highly anticipated, for instance, α-squarographite and lothographite (consisting of square C_4 and hexagon C_6), BPC (or graphenylene, composed of C_4, C_6, and dodecagon C_{12}), planar C_4 (or T graphene, structured by C_4 and octagon C_8), octite SC (containing pentagon C_5, C_6, and C_8), pentaheptite (constructed by C_5 and heptagon C_7), polycyclic net (including triangle C_3 and C_{12}), HOPG (combined by C_5, C_6, and C_7), net C and net W (assembled of C_4, C_6, and C_8), OPG-L and OPG-Z (build of C_5 and C_7), S-graphene (organized by C_4, C_6, and decagon C_{10}), and pza-C_{10} (fabricated

by C_5, C_6, and C_7).[11-26] These 2D structures are all single-atom-thick periodic carbon networks and possess tunable electronic properties (e.g., semiconducting, semimetallic with Dirac-point, and metallic). Moreover, graphene exclusively exhibits semimetallicity with zero band gap.

Another alternative approach depends on the operating multilayer graphene to realize controllable electronic characteristics. Theoretical simulations and experimental research have introduced a significant band gap in the electronic states of laminated bilayer graphene and trilayer graphene with the application of a perpendicular electric field[27-30] to relieve the band gap limitation in monolayer graphene. Bilayer graphene and trilayer graphene are *van der Walls* interaction buckled structures with a weak interlayer connection. Consequently, the crystal structures and electronic properties of covalently joined multilayer 2D carbon allotropes with ineluctable non-hexagon polygons incorporated require urgent exploration.

In this work, the structural stabilities and electronic properties of a 2D carbon allotrope called H-net with P-42m symmetry composed of squares C_4, distorted hexagons C_6, and distorted octagons C_8 are investigated by using first principle calculations. In H-net, two identical C_6+C_4+C_6 compositions cross face each other and are interlinked through distorted octagons. This configuration vividly constructs a handshake-like model. H-net is confirmed to be dynamically stable and energetically more favorable than synthesized graphdiyne and most theoretical 2D carbons at ground state. Therefore, a possible chemical synthesis from graphene nanoribbon (GNR) is proposed. H-net exhibits a semiconducting characteristic with an indirect band gap of 0.88 eV. The one-dimensional (1D) derivate nanoribbons (NRs) of H-net are tailored. The narrowest H-net NR is predicted to be metallic, whereas wider NRs

are semiconducting with increasing indirect band gaps as the width. We also explore the stabilities of H-net polymers assembled through both *van der Walls* force and covalent bonds.

2 Computational method

2D carbon ground-state structures have been extensively searched with system sizes containing up to 24 atoms/cell using the CALYPSO code.[31] The code has made successful predictions of novel carbon allotropes to explain the experimental findings.[32-34] The geometric optimization and property predictions were performed using the CASTEP code.[35] The Vanderbilt ultrasoft pseudopotential was used with the plane-wave energy cutoff of 310 eV. The exchange correlation terms were treated using the Ceperley and Alder as parametrized by Perdew and Zunger (CA-PZ) form of local density approximation (LDA).[25, 36] The Monkhorst−Pack grid parameters[37] were used to generate a k-point grid with separation of $2\pi \times 0.04$ Å^{-1}. The finite displacement method was used to calculate the phonon frequencies.

3 Results and discussion

A 2D carbon structure consisting of squares C_4, distorted hexagons C_6, and distorted octagons C_8, is proposed by using state-of-the-art theoretical tools. Fig. 1 shows two identical components (i.e., red and green C_6+C_4+C_6 units), which are also constituent elements of net W, net C, lothographite, and α-squarographite,[11, 18, 19] cross face each other and bent to arches for interconnection at the edge through folded octagons C_8 (i.e., pink sticks). These components vividly depict the handshake-like model, herein it is dubbed as H-net. The distance between opposite squares is 3.348 Å, which approaches the interlayer distance in graphite (3.400 Å). H-net is characterized by a symmetry group of P-42m with three unequal crystallographic sites occupying C1 (0.494, 0.676, 0.444), C2 (0.896, 0.564, 0.545), and C3 (0.245, 0.086, 0.517)

Wyckoff atom positions (lattice parameter *c*=30.000 Å). Atom C1 makes up the square, and atoms C1, C2, and C3 form the irregular hexagon simultaneously. Atom C3 serves as a bridge to attach the red and green independent parts. In H-net, 24 atoms share a unit cell with equivalent lattice parameter *a*=5.984 Å. Therefore, its quasi-areal density of atoms is 0.670 atoms/Å^2. The calculated areal density of graphene is 0.382 atoms/Å^2, which close to the previous value (0.379 atoms/Å^2).[18] The areal density of other 2D carbons is usually less than that of graphene because these 2D carbons are the variants of defective graphene. The density of H-net is twice that of other 2D network polymorphs. The electron density difference reveals that the C-C bonds in squares (1.439 Å and 1.538 Å) preserve the pattern of alternating double and single bonds. Bonds in hexagons are all single bonds with 1.439 Å, 1.404 Å, 1.411 Å, and 1.350 Å lengths, and bonds in octagons interlinking the red and green compositions (i.e., pink sticks) are uniformly double bonds (1.459 Å and 1.458 Å) (Fig. 1). The average bond length in H-net is 1.430 Å, which is close to that of graphene (1.420 Å), implying the sp^2-like hybridization nature. The bond angles of H-net in squares are 90°, which is highly stained. The bond angles of H-net in hexagons and octagons oscillate around 120° (119.273° and 114.185° in hexagons, and 111.135° and 117.943° in octagons).

To examine the stability of H-net, we evaluate the formation energy by $E_f = (E_{tot(2D\ carbon)}-NE_C)/N$, where $E_{tot(2D\ carbon)}$ and E_C are the total energy of a 2D carbon and an isolated carbon atom respectively and *N* is the total number of atoms in a 2D carbon unit cell at ground state along with graphdiyne, graphyne, and several other stable 2D carbon allotropes. Although H-net (E_f = -9.34 eV/atom) is metastable relative to the energetically most stable graphene (-9.96 eV/atom) as a result of the high structural strain originating from the deviated bond lengths and angles relative to

graphene, it is more favorable than synthesized graphdiyne (-9.08 eV/atom) and most stable 2D carbons, such as α-graphyne (-8.89 eV/atom), β-graphyne (-8.99 eV/atom),[7] BPC (-9.28 eV/atom), S-graphene (-9.13 eV/atom), polycyclic net (-8.90 eV/atom), α-squarographite (-8.22 eV/atom), and lithographite (-8.19 eV/atom), thus implying its preferable thermodynamic stability. To further validate the dynamic stability of H-net, the phonon spectra of H-net are calculated (Fig. 2a). The highest phonon frequency is estimated to be 1662 cm^{-1}, matching that of graphene (approximately 1600 cm^{-1}). All branches present positive frequencies, and no imaginary frequency is found around the entire Bullion zone, confirming its dynamic stability at ground state.

As high energy graphdiyne has been successfully produced in experiments, H-net is promising for fabrication in the laboratory because of its advantageous thermodynamic stability. Fortunately, diverse 2D carbon materials have become experimental realities. For example, Lahiri et al. obtained a 1D topological defect containing octagonal and pentagonal sp^2-hybridized carbon rings embedded in a perfect graphene sheet by defect engineering.[38] Kotakoski et al. obtained a one-atom-thick flat carbon membrane with a random arrangement of alternate squares, pentagons, hexagons, heptagon, and octagons by using electron irradiation on graphene.[39] This finding seriously indicates the existence of squares and octagons in 2D carbon sheets. Aside from the above possible methods, we propose another engineering route to fabricate H-net. From the x-y diagonal direction, the red (or green) component can be viewed as the narrowest twisted GNRs with armchair edges (denoted as 3-AGNRs following the conventional nomenclature)[40] interlinked through common [2+2] cycloadditions (Fig. 1a). Accordingly, we predict a possible assembly route of H-net from GNR. At the beginning of the synthesis, parallel-laid 3-AGNRs experience dehydrogenation. Then, neighboring GNRs accompanied by helical twist

along the centerline approach each other. Finally, the chains on the same layer (i.e., red and green chains or pink and blue chains) are buckled through [2+2] cycloadditions. The interlayer chains are connected through an addition reaction to form octagons. H-net is eventually formed (Fig. 3).

Graphene has a gapless electronic band structure.Bilayer graphene and trilayer graphene have an introduced gap, but a perpendicular electric field is required. New 2D carbon sheets are expected to show rich electronic properties, but most of them are metallic or have Dirac-like fermions, such as S-graphene, polycyclic net, OPG-L, OPG-Z, net W, planar C_4, pentaheptite, and HOPG.[15-18, 22-24] However, band gap is necessary for nanoelectronic devices. For comparison, the electronic band structure of graphene is also calculated. Fig. 2 shows that graphene has zero band gap with a Dirac point at *K*, similar to previous studies. H-net is semiconductive with an indirect band gap of 0.88 eV, which is close to that of BPC (0.8 eV).[13] As DFT underestimates the band gap of semiconducting carbon, hybrid function PBE0[41] implemented in the CASTEP code is adopt to more accurately calibrate the band gap and gives a value of 2.11 eV. To further clarify the origin of the band gap, we present the band decomposed charge densities of the valence band maximum (VBM) at point *M* and the conduction band minimum (CBM) at point *G* of the band structure (Fig. 4). The spatial distribution of the VBM exhibits a bonding characteristic between atoms C1-C2 and C2-C3, whereas CBM displays an antibonding character between atoms C2-C2, indicating an indirect band gap.

Structure tailoring induces various intriguing properties in graphene and other theoretical 2D carbon allotropes. Tailored GNRs with zigzag and armchair edges are all semiconducting with tunable band gap as a function of the width and edge structure.[42, 43] Metallic net W presents a width-depended metal-semiconductor

oscillating behavior when cut into NRs,[18] whereas planar C_4 and the corresponding NRs are uniformly metallic regardless of the width alteration.[16, 22, 44] Similar peculiarities are confirmed in HOPG and its derivative NRs.[17] Consequently, peculiar electronic properties are expected to be induced in H-net NRs. Fig. 5a shows the configurations of H-net NRs with width *n* belonging to 1, 2, and 3, where *n* indicates the number of repeating unit. To guarantee the handshake-like model, the smallest width of H-net NR is geared to a unit cell. Electronic band structure calculations (Fig. 5b) indicate that H-net NR with *n*=1 (1-NR) is metallic, and its band structure is similar to that of doped AGNRs except for extra energy states.[45] Therefore, properties like those of doped AGNRs are anticipated. The band structures of 2-NR, 3-NR, and 4-NR are similar to that of 1-NR, but the two bands (red lines in Fig. 5b) crossing the Fermi level upshift to conduction band bottom and downshift to valence band top, respectively, resulting in a finite indirect band gap. The gap value increases from 0.035 eV for 2-NR to 0.076 eV for 4-NR, and finally increases to 0.88 eV as *n* reaches infinity. A close inspection of the band structure reveals the presence of a gap above the Fermi level below 1.0 eV. Moreover, wider 3-NR and 4-NR have Dirac-like points on G below the Fermi level at approximately -1.25 eV.

Graphene is a fundamental block that establishes various carbon allotropes. It can round to fullerene C_{60}, roll to carbon nanotube, laminate to graphite, and further polymerize to diamond. Similarly, 2D H-net is a promising element that can assemble carbon allotropes, such as the *van der Walls* force buckled AA-graphite-like polymer-I, the covalently bonded polymer-II, and polymer-III (Fig. 6 and Table 1), which are all dynamically stable under ambient pressure (Fig. 2). Polymer-I is energetically more favorable than H-net. The distance of adjacent squares in polymer-I between neighboring handshake-like models is 3.241 Å, which is less than the interlayer

distance in graphite (3.400 Å). Polymer-II has interlayer bonding between adjacent squares that remain flat and self-bonding in half octagons, resulting in a high sp^3 hybridization proportion increasing to two-thirds. Nevertheless, squares in polymer-III are distorted, resulting in both interlayer and inner buckling with a fixed sp^3 hybridization ratio. The density of polymer-I is smaller than that of graphite. The density of polymer-II and polymer-III is between that of graphite and diamond. Graphite transforms into diamond when it is cold compressed at up to 90 GPa along the *c*-axis.[46] Similarly, polymer-I can transform into polymer-II under a less uniaxial pressure of 50 GPa perpendicular to the planes.

4 Conclusions

We demonstrated an intriguing 2D semiconducting pure carbon allotrope called H-net with P-42m symmetry by using first principle calculations. In H-net, identical constituents composed of squares C_4 and distorted hexagons C_6 are covalently connected by distorted octagons C_8, forming a handshake-like model. H-net is dynamically stable and energetically more favorable than synthesized graphdiyne and most previous 2D carbon sheets, such as α-graphyne, β-graphyne, BPC, S-graphene, polycyclic net, α-squarographite, and lithographite at ground state. Therefore, H-net is regarded as energetically viable and is probably assembled from GNRs. Different from metallic graphene and most theoretical 2D carbon allotropes, H-net is semiconducting with an indirect band gap of 0.88 eV. Further studies indicate that metallicity can be introduced when H-net is tailored into the narrowest NRs. By contrast, wider NRs exhibit semiconducting properties and the band gaps grow following the widths.

Acknowledgements

This work was supported by NBRPC (Grant No. 2011CB808205) and NSFC

(Grants Nos. 51121061, 91022029, 51332005, and 51272227).

References

1 K. S. Novoselov, A. K. Geim, S. V. Morozov, D. Jiang, Y. Zhang, S. V. Dubonos, I. V. Grigorieva, and A. A. Firsov, *Science*, 2004, **306**, 666.

2 A. K. Geim and K. S. Novoselov, *Nat. mater.*, 2007, **6**, 183.

3 D. Jose and A. Datta, *Acc. Chem. Res.*, 2013, **47**, 593.

4 D. Jose and A. Datta, *Phys. Chem. Chem. Phys.*, 2011, **13**, 7304.

5 T. K. Mandal, D. Jose, A. Nijamudheen, and A. Datta, *J. Phys. Chem. C*, 2014, **118**, 12115.

6 D. Malko, C. Neiss, F. Viñes, and A. Görling, *Phys. Rev. Lett.*, 2012, **108**, 086804.

7 Y. Y. Zhang, Q. X. Pei, and C. M. Wang, *Appl. Phys. Lett.*, 2012, **101**, 081909.

8 J. J. Zheng, X. Zhao, S. B. Zhang, and X. Gao, *J. Chem. Phys.*, 2013, **138**, 244708.

9 R. H. Baughman, H. Eckhardt, and M. Kertesz, *J. Chem. Phys.*, 1987, **87**, 6687.

10 G. Li, Y. Li, H. Liu, Y. Guo, and D. Zhu, *Chem. Commun.*, 2010, **46**, 3256.

11 M. J. Bucknum and E. A. Castro, *Solid State Sci.*, 2008, **10**, 1245.

12 H. Zhu, A. T. Balaban, D. J. Klein, and T. P. Zivković, *J. Chem. Phys.*, 1994, **101**, 5281.

13 G. Brunetto, P. A. S. Autreto, L. D. Machado, B. I. Santos, R. P. B. dos Santos, and D. S. Galvão, *J. Phys. Chem. C*, 2012, **116**, 12810.

14 D. J. Appelhans, Z. Lin, and M. T. Lusk, *Phys. Rev. B*, 2010, **82**, 073410.

15 M. Deza, P. W. Fowler, M. Shtogrin, and K. Vietze, *J. Chem. Inf. Comput. Sci.*, 2000, **40**, 1325.

16 A. N. Enyashin and A. L. Ivanovskii, *Phys. Status Solidi B*, 2011, **248**, 1879.

17 B. Mandal, S. Sarkar, A. Pramanik, and P. Sarkar, *Phys. Chem. Chem. Phys.*, 2013, **15**, 21001.

18 X.-Q. Wang, H.-D. Lib, and J.-T. Wang, *Phys. Chem. Chem. Phys.*, 2013, **15**, 2024.

19 N. Tyutyulkov, F. Dietz, K. Müllen, and M. Baumgarten, *Chem. Phys. Lett.*, 1997, **272**, 111.

20 C. Su, H. Jiang, and J. Feng, *Phys. Rev. B*, 2013, **87**, 075453.

21 Q. Song, B. Wang, K. Deng, X. Feng, M. Wagner, J. D. Gale, K. Müllen, and L. Zhi, *J. Mater. Chem. C*, 2013, **1**, 38.

22 Y. Liu, G. Wang, Q. Huang, L. Guo, and X. Chen, *Phys. Rev. Lett.*, 2012, **108**, 225505.

23 L. C. Xu, R. Z. Wang, M. S. Miao, X. L. Wei, Y. P. Chen, H. Yan, W. M. Lau, L. M. Liu, and Y. M. Ma, *Nanoscale*, 2014, **6**, 1113.

24 X. Luo, L.-M. Liu, Z. Hu, W.-H. Wang, W.-X. Song, F. Li, S.-J. Zhao, H. Liu, H.-T. Wang, and Y. Tian, *J. Phys. Chem. Lett.*, 2012, **3**, 3373.

25 J. P. Perdew and A. Zunger, *Phys. Rev. B*, 1981, **23**, 5048.

26 V. H. Crespi, L. X. Benedict, M. L. Cohen, and S. G. Louie, *Phys. Rev. B*, 1996, **53**, R13303.

27 Y. Zhang, T.-T. Tang, C. Girit, Z. Hao, M. C. Martin, A. Zettl, M. F. Crommie, Y. R. Shen, and F. Wang, *Nature*, 2009, **459**, 820.

28 K. F. Mak, C. H. Lui, J. Shan, and T. F. Heinz, *Phys. Rev. Lett.*, 2009, **102**, 256405.

29 M. F. Craciun, S. Russo, M. Yamamoto, J. B. Oostinga, A. F. Morpurgo, and S. Tarucha, *Nat. nanotechnol.*, 2009, **4**, 383.

30 C. H. Lui, Z. Li, K. F. Mak, E. Cappelluti, and T. F. Heinz, *Nat. Phys.*, 2011, **7**, 944.

31 Y. Wang, J. Lv, L. Zhu, and Y. Ma, *Comput. Phys. Commun.*, 2012, **183**, 2063.

32 M. Hu, F. Tian, Z. Zhao, Q. Huang, B. Xu, L.-M. Wang, H.-T. Wang, Y. Tian, and J. He, *J. Phys. Chem. C*, 2012, **116**, 24233.

33 Z. Zhao, B. Xu, L.-M. Wang, X.-F. Zhou, J. He, Z. Liu, H.-T. Wang, and Y. Tian, *ACS Nano*, 2011, **5**,

7226.
34 Z. Zhao, F. Tian, X. Dong, Q. Li, Q. Wang, H. Wang, X. Zhong, B. Xu, D. Yu, J. He, H.-T. Wang, Y. Ma, and Y. Tian, *J. Am. Chem. Soc.*, 2012, **134**, 12362.
35 S. J. Clark, M. D. Segall, C. J. Pickard, P. J. Hasnip, M. I. J. Probert, K. Refson, and M. C. Payne, *Z. Kristallogr.*, 2005, **220**, 567.
36 D. M. Ceperley and B. J. Alder, *Phys. Rev. Lett.*, 1980, **45**, 566.
37 H. J. Monkhorst and J. D. Pack, *Phys. Rev. B*, 1976, **13**, 5188.
38 J. Lahiri, Y. Lin, P. Bozkurt, Oleynik, II, and M. Batzill, *Nat Nanotechnol*, 2010, **5**, 326.
39 J. Kotakoski, A. V. Krasheninnikov, U. Kaiser, and J. C. Meyer, *Phys. Rev. Lett.*, 2011, **106**, 105505.
40 Y.-W. Son, M. L. Cohen, and S. G. Louie, *Nature*, 2006, **444**, 347.
41 C. Adamo and V. Barone, *J. Chem. Phys.*, 1999, **110**, 6158.
42 Y.-W. Son, M. L. Cohen, and S. G. Louie, *Phys. Rev. Lett.*, 2006, **97**, 216803.
43 V. Barone, O. Hod, and G. E. Scuseria, *Nano Lett.*, 2006, **6**, 2748.
44 X. Q. Wang, H. D. Li, and J. T. Wang, *Phys. Chem. Chem. Phys.*, 2012, **14**, 11107.
45 A. Pramanik, S. Sarkar, and P. Sarkar, *J. Phys. Chem. C*, 2012, **116**, 18064.
46 M. Hu, Z. Zhao, F. Tian, A. R. Oganov, Q. Wang, M. Xiong, C. Fan, B. Wen, J. He, D. Yu, H.-T. Wang, B. Xu, and Y. Tian, *Sci. Rep.*, 2013, **3**, 1331.

Table and Figure captions

Table 1 Space group, lattice parameters (a, b, c, Å), density (g/cm^3), atomic Wyckoff position, and ground state energy of H-net polymers relative to graphite and diamond.

Fig. 1 (a) Optimized crystal structure of H-net. H-net consists of distorted squares C_4, hexagons C_6, and octagons C_8 with three unequal carbon atoms C1, C2, and C3. (b) and (c) Electron density difference in the hexagon and the square in H-net, respectively.

Fig. 2 Phonon spectra and electronic band structures of carbon allotropes under ambient pressure. In panel (c), the blue lines descript the LDA calculation results, and the green lines descript the PBE0 calculation results. The inserts in panels (b) and (c) are the high-symmetry points in the corresponding first Brillion zone.

Fig. 3 Possible chemical synthesis route of H-net from armchair-edged graphene nanoribbons with width of 3 (3-AGNR).

Fig. 4 Band decomposed charge density of the VBM at the K-point *M* (a) and the CBM at the K-point *G* (b) for H-net. The blue, pink, and brown spheres represent the atoms C1, C2, and C3, respectively. The translucent green and purple portions represent the spatial distribution of VBM and CBM, respectively.

Fig. 5 (a) H-net nanoribbons (NRs) with widths of n=1, n=2, and n=3. (b) Electronic band structures of H-net NRs with n=1, n=2, n=3 and n=4.

Fig. 6 Optimized crystal structures of H-net polymer-I (a), polymer-II (b), and polymer-III (c).

Table 1 Space group, lattice parameters (a, b, c, Å), density (g/cm^3), atomic Wyckoff position, and ground-state energy of H-net polymers relative to graphite and diamond.

structure	space group	lattice	density	atomic positions	energy
graphite	P63/mmc (194)	2.460, 6.800	2.24	2b (0, 0, 1/4) 2c (1/3, 2/3, 1/4)	-155.531
diamond	Fd-3m (227)	3.528	3.63	8b (-1/4, 1/4, 1/4)	-155.542
polymer-I	P-42m (111)	5.984, 6.588	2.03	8o (-0.104, 0.564, 0.704) 8o (-0.506, 0.676, 0.250) 8o (-0.755, 0.086, 0.579)	-154.894
polymer-II	P-42m (111)	6.367, 4.636	2.55	8o (0.877, 0.544, 0.660) 8o (0.500, 0.680, 0.168) 8o (0.236, 0.090, 0.590)	-154.844
polymer-III	P222 (16)	6.252, 6.375, 4.164	2.88	4u (0.668, 0.499, 0.181) 4u (0.090, 0.769, 0.395) 4u (0.507, 0.336, 0.682) 4u (0.241, 0.916, 0.372) 4u (0.456, 0.117, 0.807) 4u (0.881, 0.455, 0.323)	-154.767

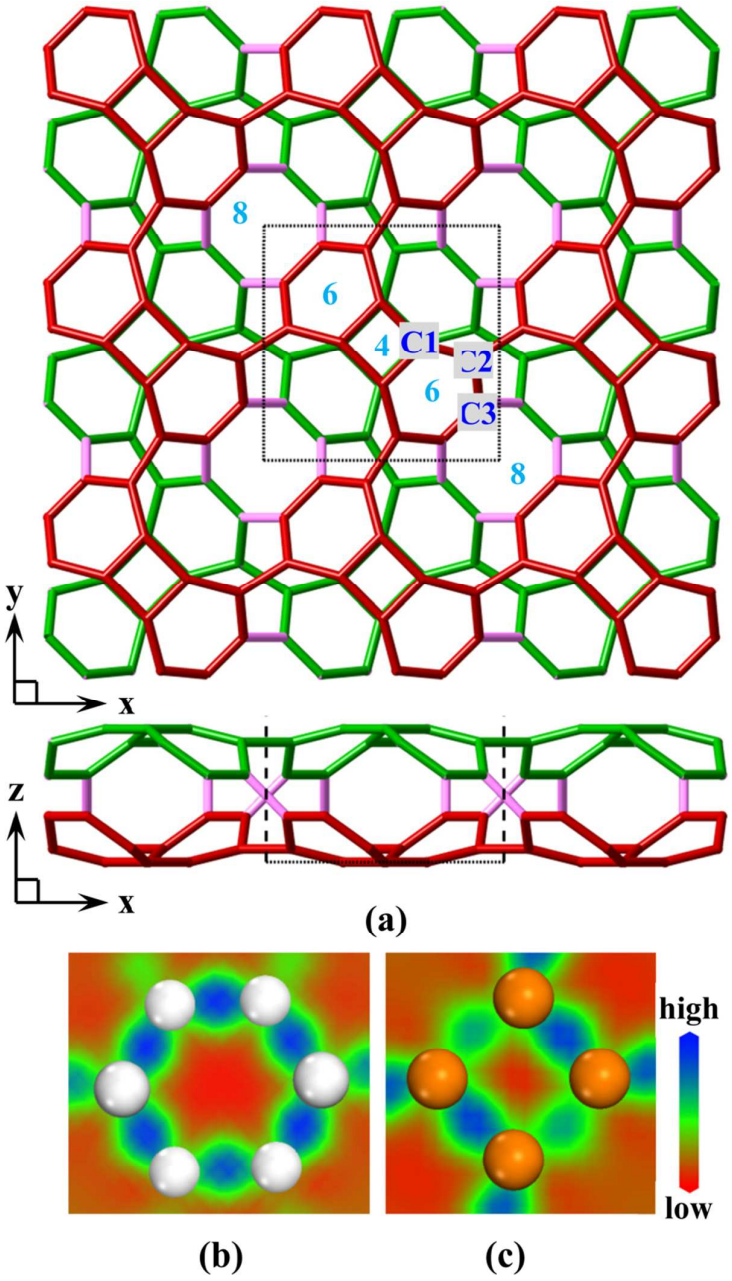

Figure 1

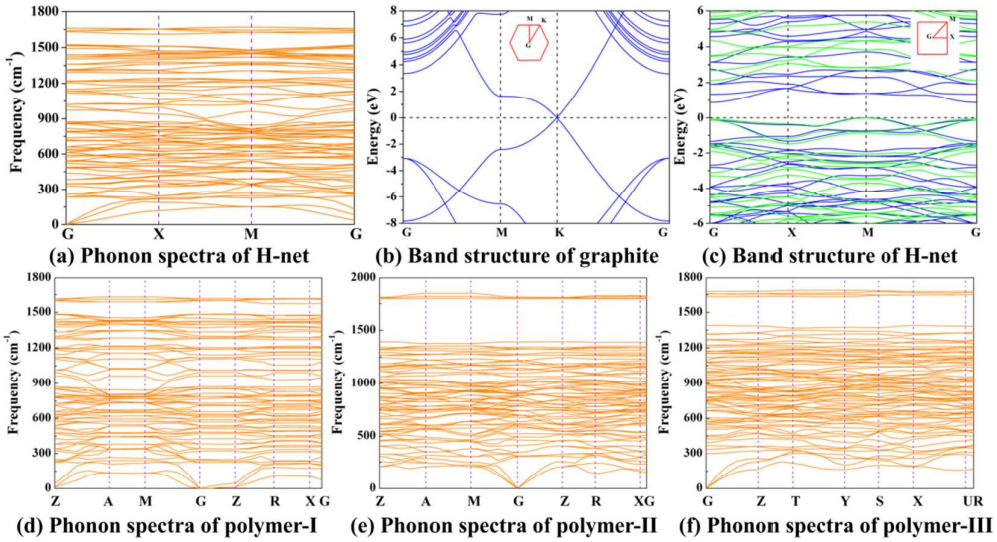

Figure 2

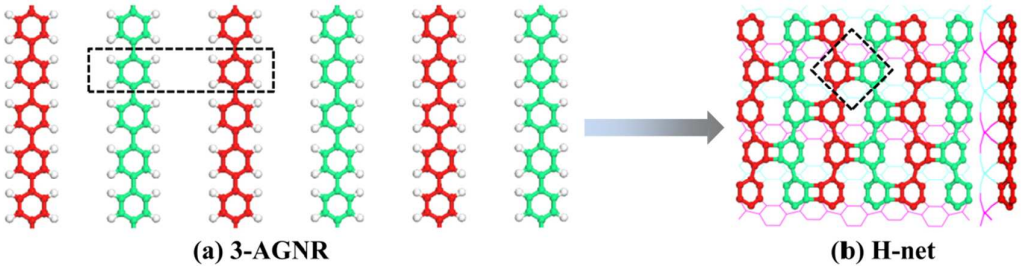

Figure 3

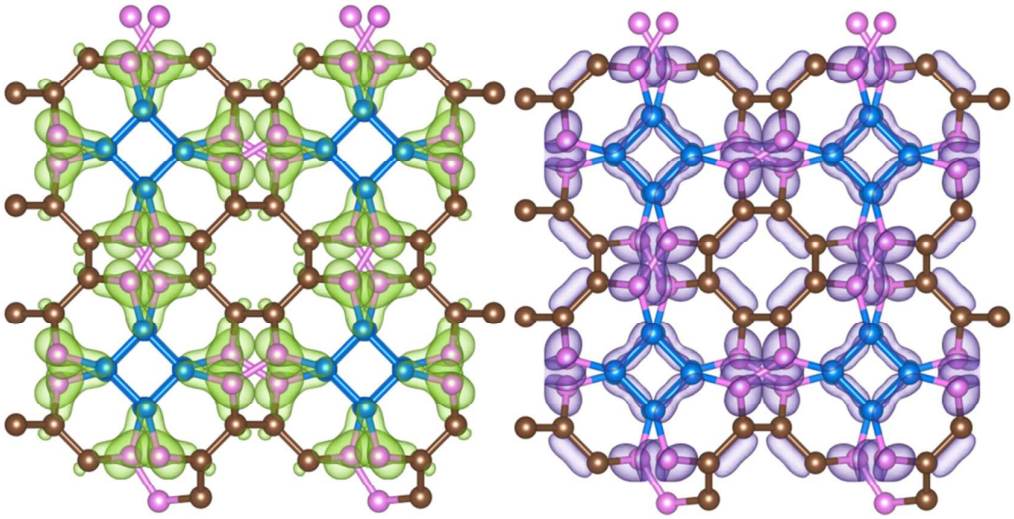

Figure 4

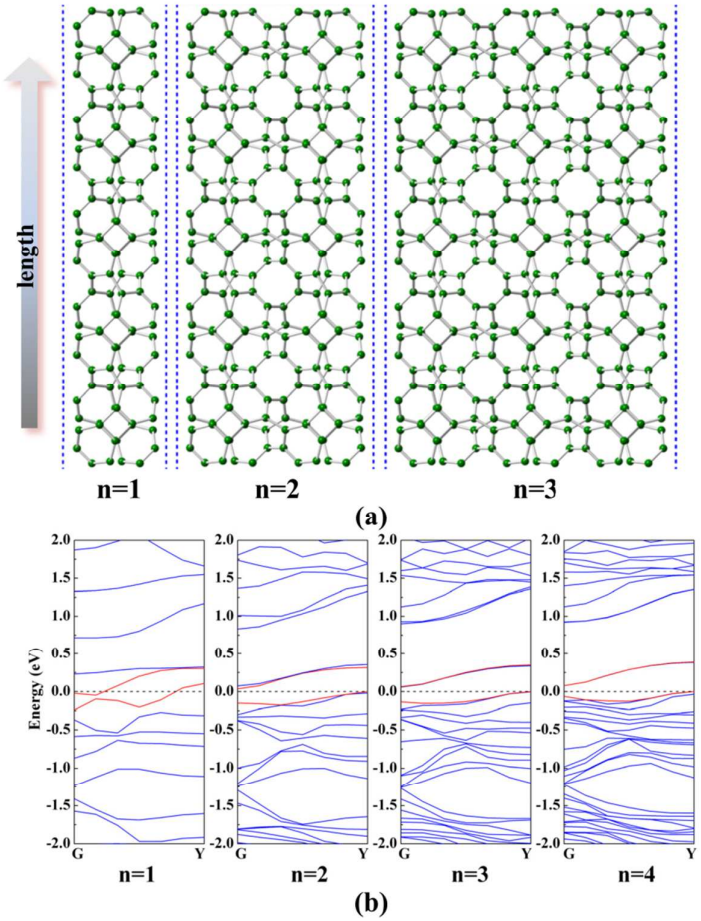

Figure 5

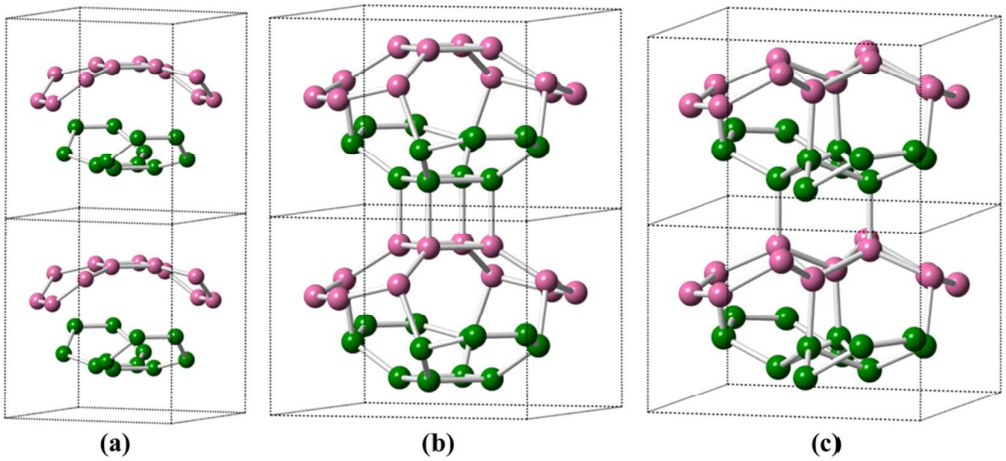

Figure 6